Supporting Information

For

Low Reorganization Energy for Electron Self-Exchange by a Formally Copper(III/II) Redox Couple

Timothy J. Zerk,[a] Caroline T. Saouma,[b] James M. Mayer,[c,*] and William B. Tolman[a,*]

[a] Department of Chemistry, Washington University in St. Louis, One Brookings Hall, Campus Box 1134, St. Louis, MO 63130-4899

[b] Department of Chemistry, University of Utah, 315 S 1400 E, Salt Lake City, UT 84112

[c] Department of Chemistry, Yale University, 225 Prospect Street, New Haven CT 06520 8107

Table of Contents

Materials and Methods

UV-vis spectra were obtained using an HP8453 (190-1100 nm) diode array spectrophotometer equipped with a Unisoku low temperature cell holder. Stopped flow measurements were performed using a TgK CryoStopped-Flow instrument equipped with a Xenon lamp and photodiode array detector in single mixing mode. The stopped-flow system was controlled by the Kinetic Studio 2.20 software and the data were analysed using ReactLab KINETICS.[1] Cyclic voltammetry (CV) experiments were performed on an EC Epsilon potentiostat from BASi using a three-electrode cell comprised of a freshly polished Pt working electrode, Pt counter electrode and non-aqueous Ag/Ag^+ reference electrode in CH_2Cl_2 with tetrabutylammonium hexaflurophosphate (TBAP) as the electrolyte and decamethylferrocene (Fc*) as the internal standard. All potentials are referenced against the ferrocenium/ferrocene ($[Fc]^{+/0}$) redox couple using the known $E_{1/2}$ (Fc*) *vs*. $E_{1/2}$ (Fc) difference in CH_2Cl_2.[2] Dichloromethane was passed over an alumina column under argon and then plumbed directly into the glovebox where it was stored over 3Å molecular sieves (20% v/v) for 24 h before use. In order to remove sieve dust, CH_2Cl_2 was also passed through a 0.3 μm syringe filter directly before use. Ferrocenium tetrakis[3,5-bis(trifluoromethyl)phenyl]borate ($[Fc][BAr_4^F]$), acetyl ferrocenium tetrakis[3,5-bis(trifluoromethyl)phenyl]borate ($[AcFc][BAr_4^F]$) and $[Bu_4N][LCuOH]$ were prepared as described.[3,4,5] The electrolyte, TBAP, was recrystalized several times from ethanol and dried overnight under high-vacuum before use. All glassware and syringes were thoroughly dried before use and solutions were prepared inside the glove-box. At least 10 mg of each reagent was measured out to minimize error due to fluctuations in the glove-box balance.

Measurement of K_{12}

The equilibrium constant (K_{12}) was initially investigated spectroscopically by titrating a CH_2Cl_2 solution of $[Bu_4N][LCuOH]$ with $[Fc][BAr_4^F]$ at −88 °C (Figure S1 **A.**). Complete oxidation required slightly more than a stoichiometric equivalent of $[Fc]^+$ (Figure S1 **B.**). The additional 'feature' which appears at ~620 nm with excess oxidant is the $[Fc]^+$ signal (Figure S2 **B.**). A parallel oxidation was performed with the much more powerful oxidant acetylferrocenium $[^{Ac}Fc][BAr_4^F]$ to confirm the molar absorptivity of [LCuOH] at -88 °C; $E_{1/2}$ (^{Ac}Fc) = 0.27 V *vs.* $[Fc]^{+/0}$ (Figure S1 **C.**). Because the oxidation of $[LCuOH]^-$ by $[Fc]^+$ is nearly stoichiometric, titration curves in the forward direction are subject to large uncertainties and thus the equilibrium was approached from the opposite direction.

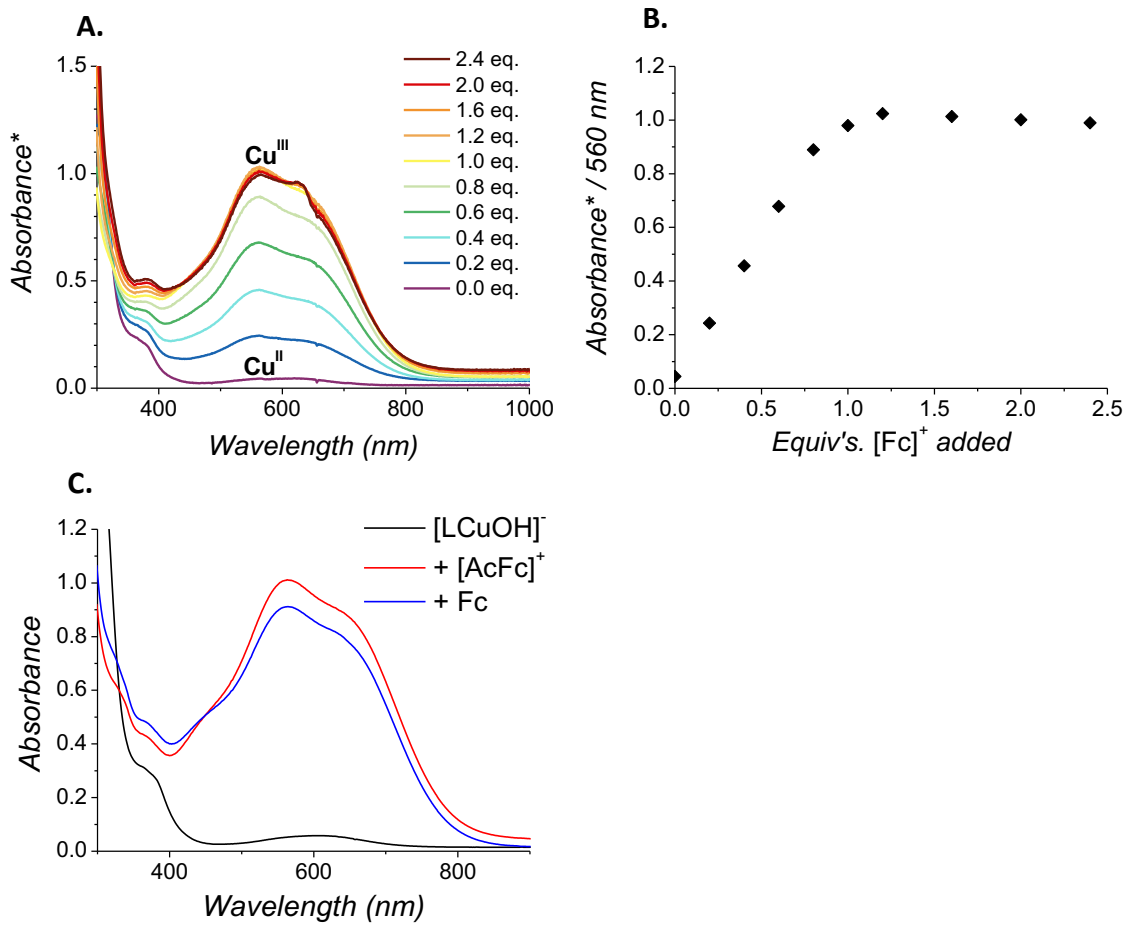

Figure S1. A. UV-vis titration of 0.1 mM [Bu_4N][LCuOH] with 4.0 mM [Fc][BAr_4^F] at −88.0 °C in CH_2Cl_2. Note: Absorbance* is the measured Absorbance which has been volume-corrected to 2.0 mL (See footnote 1). **B.** Plot following the titration in **A** at 560 nm. **C.** UV-vis spectra of 0.10 mM [Bu_4N][LCuOH] (Black curve); after adding 1.0 equivalent of [AcFc][BAr_4^F] (Red curve); after subsequently adding an equivalent of Fc (Blue curve). Data collected at −88.0 °C in CH_2Cl_2.

The equilibrium constant K_{12} for the cross reaction between $[LCuOH]^-$ and $[Fc]^+$ was therefore determined from a 'reverse' titration of Fc into a cell containing LCuOH prepared *in situ* from 0.1 mM [Bu_4N][LCuOH] and 0.1 mM [Fc][BAr_4^F] (Figure S2. **A**). The working cuvette was maintained at temperature (-88 °C) for a minimum of four minutes before making each measurement to ensure that thermal equilibrium had been reached. Initially, 1.0 mL of CH_2Cl_2 was added to the working cuvette which was used to blank the instrument. Next, 0.5 mL of a 0.4 mM stock solution of [Bu_4N][LCuOH] was added to the cuvette (final concentration of Cu^{II} ~ 1.3 mM) and a spectrum was collected (Figure S2. **A**, black curve). Next, 0.5 mL of a 0.4 mM stock solution of [Fc][BAr_4^F] was added and the spectrum of the resulting complex LCuOH was measured (red curve). After 10 min, the spectrum of LCuOH was essentially unchanged indicating negligible reduction or degradation. Finally, 50 µL aliquots of a 4.0 mM stock solution of Fc were added (2.0×10^{-7} moles, one equivalent per aliquot), leading to a decrease in the Cu^{III} signal at λ_{max} = 560 nm. At the concentrations used in this experiment, Fc and $[Fc]^+$ have

[1] Volume correction applied as follows: Absorbance* = Absorbance (measured) × (total cell volume (L)/0.002L)

negligible contributions to the absorbance at 560 nm (Figure S2. **B**). The molar absorbance of LCuOH is also ~ 25 times that of $[LCuOH]^-$ at 560 nm (Figure S1. **A**). Therefore, the equilibrium constant (K_{12}) was estimated from eq. S1 using Abs. (560 nm) as a direct measure of [LCuOH] under the assumption that all other species provided negligible contribution to the absorbance at this wavelength.

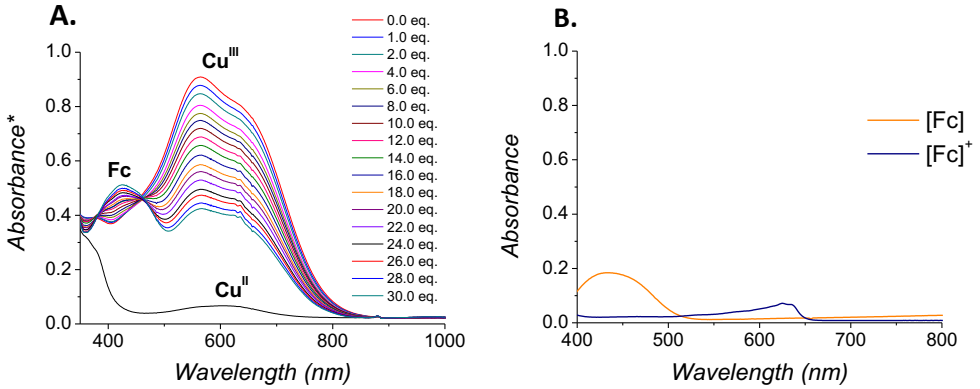

Figure S2. A. UV-vis titration of 0.10 mM LCuOH + 0.1 mM [Fc][BAr_4^F] (red curve – top) with 4.0 mM Fc at -88.0 °C in DCM. Note: Absorbance* is the measured Absorbance which has been volume-corrected to 2.0 mL. **B.** UV-vis spectra of 0.1 mM [Fc][BAr_4^F] (blue) and 1.7 mM Fc (orange) in DCM at -88 °C. These spectra represent the contributions of Fc and $[Fc]^+$ to the spectrum in Figure S2. **A** at the end of the titration.

***NOTE**:* For the remainder of this section only, charges are included inside the square brackets because concentrations are being discussed. Everywhere else throughout the SI and the maintext charges are placed outside the square brackets in accordance with IUPAC recommendations because the text is referring to the identity of a species rather than its concentration.

$$K_{12} = \frac{[\mathrm{LCuOH}][\mathrm{Fc}]}{[\mathrm{LCuOH^-}][\mathrm{Fc^+}]}$$

$$K_{12} = \frac{[\mathrm{LCuOH}][\mathrm{Fc}]}{([\mathrm{Fc^+}])^2} \qquad \text{eq. S1}$$

$$[\mathrm{Fc^+}] = [\mathrm{LCuOH}]_0 - [\mathrm{LCuOH}] \qquad \text{eq. S2}$$

$$[\mathrm{Fc}] = [\mathrm{Fc}]_0 - ([\mathrm{LCuOH}]_0 - [\mathrm{LCuOH}]) \qquad \text{eq. S3}$$

$$[\mathrm{LCuOH}] = \mathrm{Abs}_{560\mathrm{nm}}/\varepsilon_{[\mathrm{LCuOH^-}]} \qquad \text{eq. S4}$$

In equation S1, '[LCuOH]' is the concentration Cu^{III} after the solution is titrated with Fc and allowed to come to equilibrium – determined from Beer's law (equation S4). The concentration of Fc in the cell after equilibrium has been reached '[Fc]' is equal to the concentration before equilibration '$[Fc]_0$' minus the difference between $[LCuOH]_0$ and [LCuOH] (eq. S2). In equation S2, '$[LCuOH]_0$' is the initial concentration of LCuOH corrected for dilution by the Fc solution. Equation S1 was used to determine K_{12} from each of the 16 sequential spectra presented in Figure S2 **A**. The average value K_{12} = 400 is

consistent with the observation that slightly more than a single equivalent of ferrocenium is required to fully oxidize $[LCuOH]^{-}$. The experiment was repeated twice to obtain the final value K_{12} = 400 (± 50) at -88 °C.

Measurement of k_{12}

The stopped flow system was thermally equilibrated for 30 – 60 min prior to kinetic runs and the lines were thoroughly flushed with dry CH_2Cl_2. The system was blanked with dry CH_2Cl_2 at -88 °C prior to initiating experiments. Solutions of 0.2 mM $[Bu_4N][LCuOH]$ and 0.2 mM $[Fc][BAr_4^F]$ in CH_2Cl_2 were prepared in the glovebox. The reagents were loaded into gas-tight syringes (Hamilton or SGE), which were attached to gas-tight 2-way valves (SGE). The individual stopped-flow lines were rinsed with reagent prior to making the shots and the first two shots were omitted. Mixing produced a solution containing 0.1 mM concentrations of both reagents. Spectra were collected between 400 – 800 nm every 1.7 ms after mixing (Figure S3 **A.**). Global analysis of the data using ReactLab KINETICS provided an excellent fit using a simple, second order reaction mechanism (Figure S3 **B.**). The second order rate constant reported in Table 1 in the main text is obtained as an average from the fit of four separate experiments (Table S1).

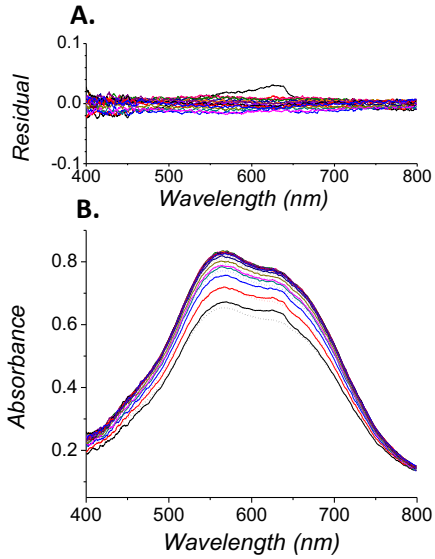

Figure S3. A. Absorbance differences ('Residuals') between the experimental and fitted spectra for each of the time-dependent spectra shown in **B**. **B.** Overlay of experimental (solid curves) and fitted spectra (dotted curves) during the stopped-flow mixing of 0.1 mM $[LCuOH][Bu_4N]$ and 0.1 mM $[Fc][BAr_4^F]$ at −88 °C in CH_2Cl_2. Fitted spectra generated from ReactLab KINETICS using a second order model.

Table S1. Rate constants (k_{12}) determined from four individual measurements at −88 °C in CH_2Cl_2.

Experiment #	**k_{12} (M^{-1} s^{-1})**
1	6.2×10^7
2	5.7×10^7

3	6.2×10^7
4	5.2×10^7

Application of the Marcus Equation

In the Marcus model, an electron transfer (ET) reaction is considered to proceed *via* initial formation of a weak precursor complex "**P**" with an equilibrium constant K_P, which then undergoes ET to give the successor complex ("**S**") that dissociates (K_S^{-1}, Scheme S1). The second-order rate constant (k_{12}) measured for the reaction of $[LCuOH]^-$ with $[Fc]^+$ to yield LCuOH is equal to $K_p k_{12}$'.

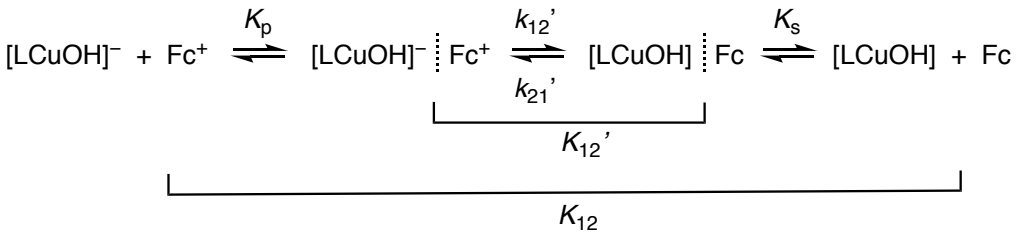

Scheme S1. Mechanism for cross-reaction between $[LCuOH]^-$ and Fc^+.

The self-exchange rate constant (k_{11}) for LCuOH/$[LCuOH]^-$ ET is estimated from the Marcus cross-relation,[6] which can be rearranged to give eq. S5. In this equation, k_{22} is the rate constant for $[Fc]^+$/Fc ET self-exchange, k_{12} is the rate constant for the ET cross reaction (Scheme S1), K_{12} is the equilibrium constant, W_{12} is a term associated with the work required to bring the reactants/products together in the precursor/successor complexes (*vida infra*), and f_{12} is a known function of k_{11}, k_{12}, K_{12}, and the individual work terms for the cross- and self-exchange reactions (eq. S5). Equation S5, which is the typical 'cross-relation', can be rearranged to eq. S6 for the purposes of our analysis.

$$k_{12} = \sqrt{k_{11} k_{22} K_{12} f_{12}}\, W_{12} \qquad \text{eq. S5 (equation 2 in the main text).}$$

$$k_{11} = \left(\frac{k_{12}}{W_{12}}\right)^2 \left(\frac{1}{k_{22} f_{12} K_{12}}\right) \qquad \text{eq. S6}$$

As $[LCuOH]^-$ and $[Fc]^+$ are oppositely charged species, there is an electrostatic attraction that makes formation of the precursor complex favorable ($K_P \approx 500$ M^{-1}, see below). In contrast, there is no such attraction in the successor complex of two neutral species, so $K_P \neq K_S$. Since $K_{12} = K_P K'_{12}/K_S$, this implies that $K_{12} \neq K_{12}'$. In other words, the driving force for the unimolecular ET step, $\Delta G^{\circ\prime} = -RT\ln(K'_{12})$, is different from the overall (bimolecular) driving force to form separated ions, $\Delta G^\circ = -RT\ln(K_{12})$. The corrected free energy change ($\Delta G^{\circ\prime}$) is given by Equation S7, from which K_{12}' is obtained ($K_{12}' = \exp(-\Delta G^{\circ\prime}/RT)$).

$$\Delta G^{o\prime} = \Delta G^o + w_{21} - w_{12} \qquad \text{eq. S7}$$

In eq. S7, w_{12} corresponds to the electrostatic work term for bringing $[LCuOH]^-$ and $[Fc]^+$ to the mean distance for ET, and w_{21} corresponds to the electrostatic work term for bringing [LCuOH] and [Fc] to the mean distance for ET (for the reverse reaction).[6] The electrostatic work terms can be estimated from eq. S8,[7] where Z_1 and Z_2 are the charges on the species to be oxidized and reduced, respectively, e is the elementary charge (e^2 = 332.1 kcal Å mol^{-1}), f is the Debye screening factor that defines the effect of ionic strength, D is the static dielectric constant of the solvent, and r_{12} is the center-to-center distance between contacting reagents.

$$w_{12} = \frac{Z_1 Z_2 e^2 f}{D r_{12}} \qquad \text{eq. S8}$$

The Debye screening factor is given by eq. S9, where k_B is Boltzmann's constant, μ is the ionic strength (M), and T is temperature (K).

$$f = \left\{1 + r_{12}\sqrt{\frac{8\pi e^2 \mu}{10^{27} D k_B T}}\right\}^{-1} \qquad \text{eq. S9}$$

For the reaction of $[LCuOH]^-$ with $[Fc]^+$, r_{12} is taken as half the sum of the radii of $[LCuOH]^-$ and $[Fc]^+$, or 8.5 Å. The radius of $[LCuOH]^-$ was taken to be 5.5 Å, which corresponds to ½ the shortest Cu-Cu distance in the solid-state structure of $[LCuOH]^-$.[5] The radius of $[Fc]^+$ was taken to be 3 Å, which is that of Fc.[8] The static dielectric constant of CH_2Cl_2 has been measured across a wide range of temperatures (Figure S4);[9] D_{CH2Cl2} at −88 °C was interpolated from this data (= 15.75).

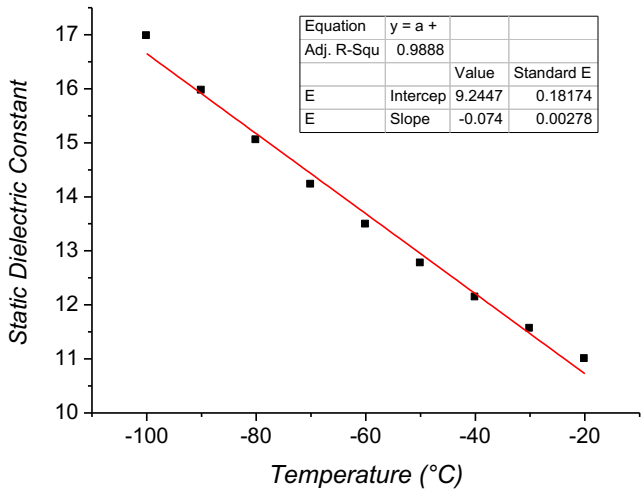

Figure S4. Plot of static dielectric constant *vs*. temperature for CH_2Cl_2. Experimental data – squares,[9] linear fit (performed here for interpolation purposes) - red line.

The Debye screening factor for the reaction in CH_2Cl_2 of 0.1 mM $[LCuOH]^-$ with 0.1 mM $[Fc]^+$, at ionic strength μ = 0.0002 M, is 0.95. The electrostatic work term, w_{12}, for bringing $[LCuOH]^-$ and $[Fc]^+$ to the mean distance for ET is thus calculated as –2.3 kcal mol^{-1} in CH_2Cl_2. Note the work term for the reverse reaction, w_{21}, and for the self-exchange reactions, w_{11} and w_{22}, are all equal to zero because in each case at least one of the ET partners has a charge of zero. The work terms w_{12} and w_{21} are the standard way to estimate K_p and K_s, respectively ($K_p \approx \exp(-w_{12}/RT)$) and $K_s \approx \exp(-w_{21}/RT)$).[7] Thus, $K_p \approx 550$ and $K_s \approx 1$.

W_{12} is defined by eq. S10.[6]

$$W_{12} = exp\left(\frac{-(w_{12}+w_{21}-w_{11}-w_{22})}{2RT}\right) \quad \text{eq. S10}$$

Substituting the work terms leads to $W_{12} = 23$. The f_{12} term of eq. S6 is defined by equation S11.[6]

$$f_{12} = exp\left[0.25\frac{\left(ln\,K_{12}+\frac{w_{12}-w_{21}}{RT}\right)^2}{ln\left(\frac{k_{11}k_{22}}{Z^2}\right)+\frac{w_{11}+w_{22}}{RT}}\right] \quad \text{eq. S11}$$

In equation S11, Z is the collision frequency, taken to be 10^{11} $M^{-1}s^{-1}$.[6,10] For the system in consideration, this simplifies to eq. S12 because many of the work terms are zero.

$$f_{12} = exp\left[0.25\frac{\left(ln\,K_{12}+\frac{w_{12}}{RT}\right)^2}{ln\left(\frac{k_{11}k_{22}}{Z^2}\right)}\right] \quad \text{eq. S12}$$

$$f_{12} = exp\left[\frac{2.68\times10^{-1}}{ln(k_{11}5.64\times10^{-17})}\right]$$

Rearrangement of eq. S6 and plugging in values for k_{12}, k_{22}, K_{12}, and W_{12} gives equation S13. The self-exchange rate constant for Fc^+/Fc (k_{22}) at −88 °C in CH_2Cl_2 is 5.6×10^5 M^{-1} s^{-1}.[11] A simultaneous solution of eq. S12 and S13 gives a value of 3×10^4 M^{-1} s^{-1} for k_{11}. Then, from equation S12, f_{12} is calculated to be 1.0, as is typical.

$$f_{12}k_{11} = \left(\frac{k_{12}}{W_{12}}\right)^2\left(\frac{1}{k_{22}K_{12}}\right) \quad \text{eq. S13}$$

$$f_{12}k_{11} = 7.10 \times 10^3$$

The rate constant for ET self-exchange is related to the free energy of activation (ΔG^*) (eq. S14) and directly to the reorganizational energy, λ (eq. S15, in the adiabatic limit).[6]

$$k_{11} = Z\,exp\left(\frac{-\Delta G^*}{RT}\right) \quad \text{eq. S14}$$

$$\Delta G^* = w_{11} + \frac{\lambda}{4}\left(1 + {\Delta G^{o\prime}}/{\lambda}\right)^2 \quad \text{eq. S15}$$

For self-exchange, $\Delta G^{o'}$ is zero, and w_{11} is zero for the LCuOH/[LCuOH]$^-$ self-exchange, so eq. S14 can be expressed as equation S16. From the calculated value of k_{11}, a reorganization energy of 0.95 (± 0.17) eV or 22 (± 4) kcal mol^{-1} is calculated in CH_2Cl_2.

$$k_{11} = Z\, exp\left(\frac{-\lambda}{4RT}\right) \qquad \text{eq. S16 (eq. 1 in the main text)}$$

The total reorganization energy λ is the sum of the inner- and outer-sphere reorganization energies (λ_i and λ_o, respectively; eq. S17).

$$\lambda = \lambda_i + \lambda_o \qquad \text{eq. S17 (eq. 3 in the main text)}$$

The outer-sphere reorganization energy can be calculated according to the dielectric continuum model described by eq. S18 which assumes a hard sphere model for the reagents.

$$\lambda_o = (\Delta e)^2 \left[\frac{1}{2a_1} + \frac{1}{2a_2} - \frac{1}{r}\right]\left[\frac{1}{D_{opt}} - \frac{1}{D_{stat}}\right] \qquad \text{eq. S18 (eq. 4 in the main text)}$$

The term Δe is the elementary charge transferred (= √(1.4399764 MeV•fm) for the self-exchange reaction in consideration), a_1 and a_2 are the individual radii of the two components involved in the reaction which in this case is estimated to be 0.55 nm (*vide supra*) for both LCuOH and [LCuOH]$^-$, r is the centre-to-centre separation distance (= 1.1 nm), D_{stat} is the static dielectric constant taken as 15.75 (*vide supra*), and D_{opt} is the optical dielectric constant. The optical dielectric constant D_{opt} is approximated as the square of the refractive index. The temperature-dependent refractive index of CH_2Cl_2 has been measured.[12] Here we extrapolated this data to −88 °C to obtain a refractive index of 1.496 (Figure S5); thus, D_{opt} is approximately 2.238. Substituting the relevant values into equation S18 yields an outer sphere reorganization energy λ_o of 0.50 eV and therefore an inner sphere reorganization energy λ_i of 0.45 eV for the LCuOH/[LCuOH]$^-$ ET self-exchange reaction.

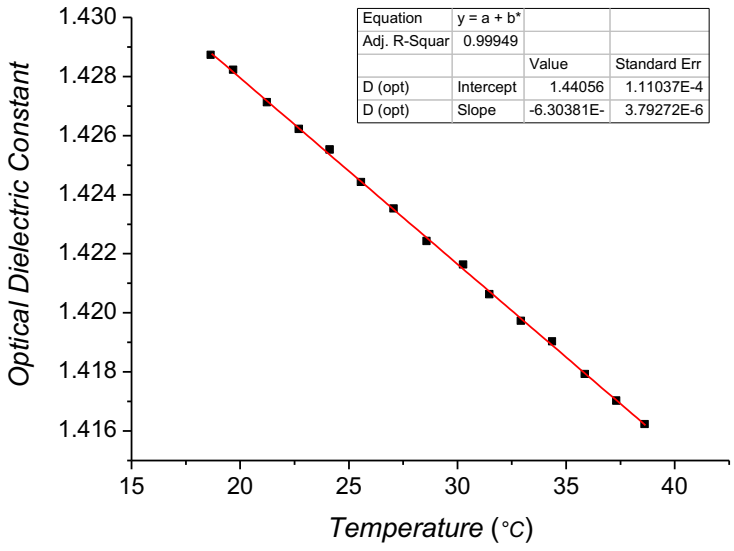

Figure S5. Plot of refractive index *vs*. temperature for CH_2Cl_2.[12] Experimental data – circles, linear fit - black line.

Effect of solvent on λ_o

From the following analysis, we conclude that differences in solvent, while important, are not the key variable in tuning the reorganization energy across the wide range observed in Figure 4 of the main text. According to the Marcus theory, for complexes which are coordination number invariant during the self-exchange reaction, the principal effect of the solvent is on the outer-sphere reorganization energy λ_o. Taking CH_2Cl_2 and water as examples of non-polar and polar solvents, respectively, and $[Cu^{II}(UN\text{-}O^-)(O_2^{\bullet-}/O_2^{2-})]^{2+}$ as a model which has been characterized crystallographically,[15] eq. S18 can be used to calculate λ_o at 25 °C using known static and dielectric constants. At 25 °C, D_{opt} for DCM is calculated to be 1.424 from Figure S5 (the square of the refractive index), and D_{stat} is calculated to be 7.378 from Figure S4. The static dielectric constant of water (D_{stat}) has been measured as 78.46 at room temperature and pressure[13] and D_{opt} is calculated as 1.803 under the same conditions by squaring the average of the measured values of the refractive index at 20 °C and 30 °C.[14] The radius of $[Cu^{II}(UN\text{-}O^-)(O_2^{\bullet-})]^{2+}$ (a_1) = the radius of $[Cu^{II}(UN\text{-}O^-)(O_2^{2-})]^+$ (a_2) = 0.6775 nm[15] and $r = a_1 + a_2$. Substituting the respective values into eq. S18 leads to λ_o = 0.33 eV (CH_2Cl_2) and λ_o = 0.58 eV (water). At −88 °C, D_{stat} = 15.75 in DCM and D_{opt} = 2.238 in CH_2Cl_2 leading to λ_o = 0.41 for the same superoxide complex. Thus, differences in solvent are not the principal reason for the distribution of the λ values in Table 2 or Figure 4 of the main text.

Measurement of ΔS°_{rxn}

Cyclic voltammetry was performed on solutions containing 1.0 mM $[Bu_4N][LCuOH]$, 0.5 mM Fc*, and $[Bu_4N][PF_6]$ electrolyte. Solutions were prepared and added to the electrochemical cell inside the glovebox and the cell was sealed with parafilm before rapid transfer outside the box to a temperature-controlled water bath where an argon gas source constantly purged the atmosphere above the solution. The temperature was controlled by immersing the 20 mL cell in an NaCl/ice/water bath or plain water bath ensuring that the working solution in the cell was submerged below the water level of the bath. The solution in the cell was stirred for 5 min at each temperature before recording a voltammogram to ensure that thermal equilibrium had been reached. A sweep rate of 50 mV s^{-1} was selected because this yielded reversible voltammetry which is essential for temperature-dependent studies; $|i_{pa}/i_{pc}| \sim 1.0$ for the $Cu^{III/II}$ and $Fe^{III/II}$ redox couples at 50 mV s^{-1}. At each temperature, three or four independent voltammograms were recorded. Each point in Figure 3B of the main text is an average of these four measurements. The temperature-dependent voltammetry experiments were also repeated twice to ensure a robust value of ΔS° was obtained. The electrode was polished, rinsed and dried before each scan; this was important to avoid fouling on the electrode surface leading to spurious results. The temperature-dependent voltammetry was measured at 0.2 M TBAP (Figure 3a of the main text) 1.0 M TBAP (Figure S6. **A**.). The temperature-dependent redox potentials are plotted for both experiments in

Figure S6. **B**. The raw data for both experiments are collected in Tables S2 and S3. The redox potential of [Bu_4N][LCuCl] was also measured in CH_2Cl_2 (0.2 M TBAP, 298 K) and is shown in Figure S7; $E_{1/2}$ = 0.338 V *vs*. $Fc^{+/0}$.

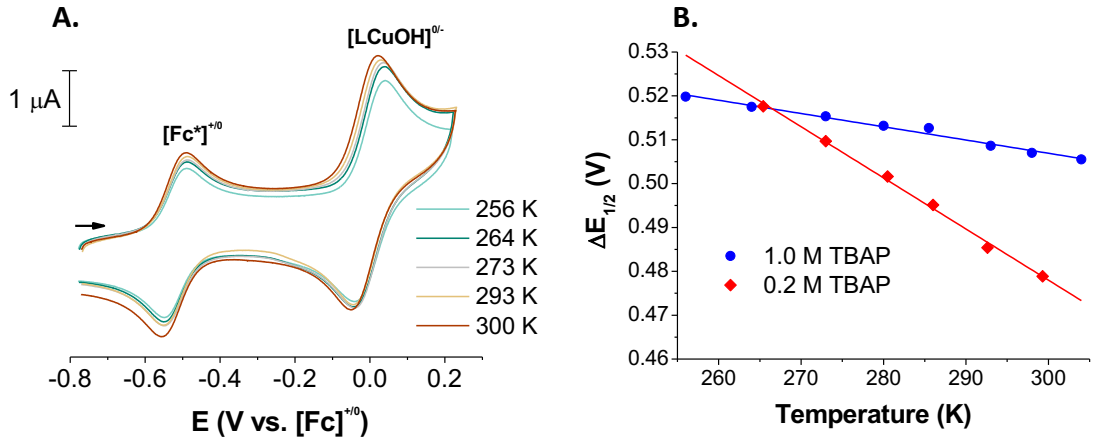

Figure S6. **A**. Illustrative temperature-dependent cyclic voltammograms of [Bu_4N][LCuOH] (1.0 mM) + [Fc*] (0.5 mM) in CH_2Cl_2. I = 0.2 M [$Bu_4N.PF_6$]; sweep rate = 50 mV s^{-1}. **B.** Plot of $\Delta E_{1/2}$ vs. T, where $\Delta E_{1/2} = E_{1/2}$ (Cu) – $E_{1/2}$ (Fc*) (same as Figure 3B in the text).

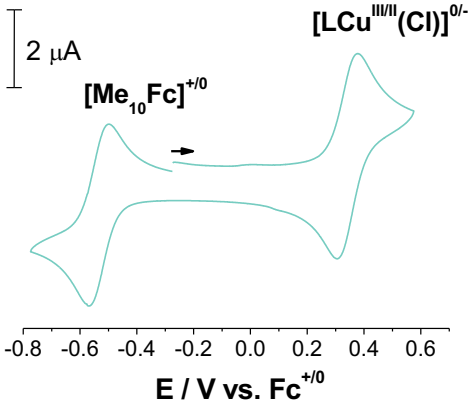

Figure S7. Cyclic voltammetry of 1.0 mM [LCuCl][Bu_4N] and 0.5 mM [Fc*] in DCM at 298K. 0.2 M TBAP, Pt working electrode. Sweep rate – 50 mV s^{-1}. *Note*: $[Fc^*]^{+/0}$ potential adjusted to -540 mV vs. $[Fc]^{+/0}$ (*vida supra*).

Table S2. Temperature-dependent redox potentials measured on a solution of 1.0 mM [LCuOH][Bu_4N] and 0.5 mM decamethylferrocene [Fc*] in DCM at 50 mV s^{-1}. 0.2 M TBAP. Potentials are referenced to $[Fc]^{+/0}$.

Temp (°C)	$E_{1/2}$ / V $[Fc^*]^{+/0}$	$E_{1/2}$ / V $[Cu^{III/II}]^{0/-}$	$\Delta E_{1/2}$ / V	Temp (°C)	$E_{1/2}$ / V $[Fc^*]^{+/0}$	$E_{1/2}$ / V $[Cu^{III/II}]^{0/-}$	$\Delta E_{1/2}$ / V
-7.6	-0.545	-0.030	0.5155	13.1	-0.542	-0.048	0.494
-7.6	-0.545	-0.027	0.519	13.1	-0.542	-0.048	0.4945
-7.6	-0.545	-0.027	0.519	13.1	-0.542	-0.046	0.496
-7.6	-0.545	-0.029	0.517	19.6	-0.541	-0.056	0.4855
-0.2	-0.544	-0.035	0.5095	19.6	-0.541	-0.055	0.4865
-0.2	-0.544	-0.034	0.51	19.6	-0.541	-0.056	0.4855
-0.2	-0.544	-0.035	0.5095	19.6	-0.541	-0.057	0.484
7.5	-0.543	-0.044	0.4995	26.3	-0.540	-0.062	0.478
7.5	-0.543	-0.041	0.5025	26.3	-0.540	-0.061	0.4795
7.5	-0.543	-0.042	0.5015	26.3	-0.540	-0.060	0.4805
7.5	-0.543	-0.040	0.503	26.3	-0.540	-0.063	0.4775
13.1	-0.542	-0.046	0.496				

Table S3. Temperature-dependent redox potentials measured on a solution of 1.0 mM [LCuOH][Bu_4N] and 0.5 mM decamethylferrocene [Fc*] in DCM at 50 mV s^{-1}. 1.0 M TBAP. *Note:* Potentials are uncorrected versus the Ag^+/Ag wire reference electrode.

Temp (°C)	$E_{1/2}$ / V $[Fc^*]^{+/0}$	$E_{1/2}$ / V $[Cu^{III/II}]^{0/-}$	$\Delta E_{1/2}$ / V	Temp (°C)	$E_{1/2}$ / V $[Fc^*]^{+/0}$	$E_{1/2}$ / V $[Cu^{III/II}]^{0/-}$	$\Delta E_{1/2}$ / V
-17.0	-0.547	-0.021	0.526	12.5	-0.542	-0.032	0.5105
-17.0	-0.547	-0.028	0.519	12.5	-0.542	-0.029	0.5135
-17.0	-0.547	-0.033	0.5145	20.0	-0.541	-0.033	0.508
-9.0	-0.546	-0.028	0.5175	20.0	-0.541	-0.033	0.5085
-9.0	-0.546	-0.032	0.5135	20.0	-0.541	-0.032	0.509
-9.0	-0.546	-0.035	0.511	20.0	-0.541	-0.032	0.509
0.0	-0.544	-0.027	0.517	25.0	-0.540	-0.034	0.5065
0.0	-0.544	-0.032	0.512	25.0	-0.540	-0.035	0.505
0.0	-0.544	-0.027	0.517	25.0	-0.540	-0.031	0.5095
7.0	-0.543	-0.027	0.516	31.0	-0.539	-0.033	0.506
7.0	-0.543	-0.033	0.5105	31.0	-0.539	-0.035	0.504
7.0	-0.543	-0.030	0.513	31.0	-0.539	-0.033	0.5065
12.5	-0.542	-0.028	0.514				

Approximating E° by $E_{1/2}$

For a reversible redox reaction with no associated chemical reaction/s, the formal potential (E^{θ}) at a planar electrode is related to the half-wave potential ($E_{1/2}$) by equation (S19).[16]

$$E_{1/2} = E^0 - \frac{RT}{nF}\ln\left(\frac{D_{ox}}{D_{red}}\right) \quad (eqn.\,\mathrm{S19})$$

If the diffusion coefficients of the oxidised and reduced forms of the analyte are equal, eqn. S19 reduces to the form $E_{1/2} \sim E^{\theta}$. In this work, the diffusion coefficients of the copper and decamethylferrocene/ferrocenium complexes were determined using the Randles-Sevich equation (eqn. S20);[17]

$$i_p = 0.4463nF\mathrm{AC}\left(\frac{nFvD}{RT}\right)^{1/2} \quad (eqn.\,\mathrm{S20})$$

Here the peak current 'i_p' (in Amps) of either the cathodic or anodic sweep is related to the number of electrons involved in the reduction/oxidation (n), the electrode area (A - in cm^2), the scan rate (v - in V s^{-1}), the concentration of analyte at the commencement of the sweep (C*- in mol cm^{-3}), the cell temperature (T – in K) and the gas constant (R - in J mol^{-1} K^{-1}). Table S4 collects the peak currents and associated diffusion rates for the copper and decamethylferrocene/ferrocenium complexes across the range of temperatures measured in Figure 3 of the main text. Substituting these diffusion coefficients into eqn. S19 leads to a maximum difference of 3 mV between $E_{1/2}$ and $E°$ measured across the full range of temperatures. Since this small difference is well-inside the error margins of the $\Delta S°$ experiments, $E°$ can be approximated $E_{1/2}$.

Table S4. Peak currents and corresponding diffusion rates measured during linear sweep voltammetry of 1.0 mM [LCuOH][Bu_4N] and 0.5 mM decamethylferrocene [Fc*] in DCM at various temperatures using a Pt electrode with a surface area of 0.013 cm^2 at a sweep rate of 50 mV s^{-1}. 0.2 M TBAP.

	$[Fc^*]^{+/0}$				**$[LCu^{I}OH]^{0/-}$**			
Temp (°C)	**i_{pa} ($A \times 10^{-6}$)**	**$D_{Fe(II)}$ ($cm^2\ s^{-1}$)**	**i_{pc} ($A \times 10^{-6}$)**	**$D_{Fe(III)}$ ($cm^2\ s^{-1}$)**	**i_{pa} ($A \times 10^{-6}$)**	**$D_{Cu(II)}$ ($cm^2\ s^{-1}$)**	**i_{pc} ($A \times 10^{-6}$)**	**$D_{Cu(III)}$ ($cm^2\ s^{-1}$)**
-7.6	2.54	3.77E-05	2.60	3.95E-05	2.10	6.44E-06	2.10	6.44E-06
-0.2	2.70	4.37E-05	2.74	4.51E-05	2.10	6.62E-06	2.20	7.26E-06
7.5	2.80	4.84E-05	2.90	5.19E-05	2.20	7.47E-06	2.30	8.16E-06
13.1	3.00	5.66E-05	3.10	6.05E-05	2.40	9.06E-06	2.40	9.06E-06
19.6	3.30	7.01E-05	3.40	7.44E-05	2.70	1.17E-05	2.60	1.09E-05
26.3	3.50	8.07E-05	3.30	7.17E-05	3.00	1.48E-05	3.10	1.58E-05

Error analysis:

The following section considers the uncertainties associated with each parameter in the cross-relation (eq S5, reproduced below) and the corresponding influence this has on the calculated values of k_{11} and λ.

$$k_{12} = \sqrt{k_{11}k_{22}K_{12}f_{12}}W_{12} \qquad \text{eq. S5}$$

k_{12}:

Figure S8 illustrates the sensitivity of k_{12} which is determined from the fit of the experimental stopped-flow data presented in Figure 2 of the main text. Where k_{12} is perturbed away from the line of 'best fit' (k_{12} = 6 × 10^7 M^{-1} s^{-1} - red trace), the corresponding kinetic traces do not accurately reproduce the experimental data (diamonds). The two traces which represent the upper and lower bounds of the experimental error (4 and 8 (× 10^7 $M^{-1}s^{-1}$) – green and orange) do not accurately fit the experimental data points while the traces with a two-fold margin of error (black and blue) clearly yield poor agreement with the data. Therefore, even though the experiment only captures the final 30% of the cross-reaction, enough data is collected to determine k_{12} with reasonable certainty, 6±2 × 10^7 $M^{-1}s^{-1}$.

Figure S8 shows that the 4 × 10^7 M^{-1} s^{-1} line does not fit the data well. This value would imply that λ = 1.00 eV, within the stated uncertainty of 0.95 (± 0.17) eV, and this value provides an upper limit for λ. Thus, the conclusion that λ is unusually small is strongly supported by this analysis.

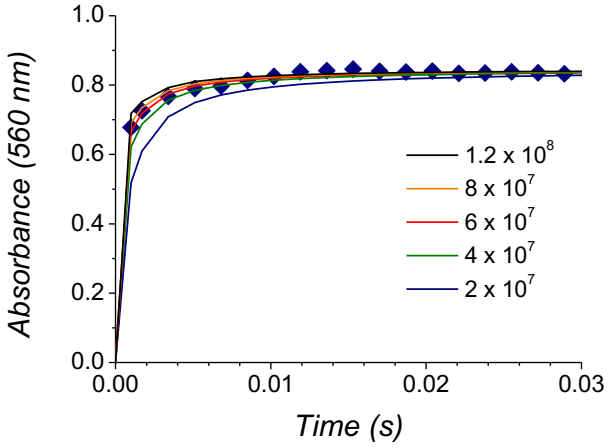

Figure S8. Sensitivity of k_{12} from Figure 2 in the main text. Diamonds are the experimental data and the red trace is the 'best fit' with k_{12} = 6 × 10^7 M^{-1} s^{-1}. The traces with k_{12} = 2 × 10^7, 4 × 10^7, 8 × 10^7 and 1.2 × 10^8 M^{-1} s^{-1} were generated using Reactlab Kinsim for comparison.[1]

Table S5. Key parameters from the Marcus cross-relation and their associated uncertainties.

Parameter	Value	Uncertainty (±)
k_{12} (-88 C)	6×10^7 $M^{-1}s^{-1}$	2×10^7 $M^{-1}s^{-1}$
k_{22}	5.6×10^5 $M^{-1}s^{-1}$	See text
K_{12}	400	50
k_{11} (-88 °C)	3×10^4 $M^{-1}s^{-1}$	8×10^4 $M^{-1}s^{-1}$
λ	0.95 eV	0.17 eV

k_{22}:

$$ln(k_{22}) = \ln(A_{ex}) - E_{act}/RT \qquad \text{eq. S21}$$

Wahl *et* al. measured the Fc^+/Fc self-exchange rate constant (k_{22}) at temperatures between 0 and 30 °C and determined the activation energy 'E_{act}' from the slope of the corresponding Arrhenius plot (logk_{22} vs. 1/T).[17] The uncertainty in E_{act} was "*estimated from the maximum and minimum slopes of lines drawn to be reasonably consistent with the data and associated uncertainties on the logk vs. 1/T plot."* E_{act} was reported as 2.0 (± 1.0) kcal mol^{-1}.

The Fc^+/Fc self-exchange rate constant extrapolated from Wahl's results to -88 °C (185 K) with E_{act} = 2.0 kcal mol^{-1} is $k_{22} = 5.6 \times 10^5$ M^{-1} s^{-1} ($\ln(k_{22}) = 13.2$). The uncertainty of ±1 kcal mol^{-1} corresponds to an uncertainty in $\ln(k_{22})$ of (±1 kcal mol^{-1})/RT = 2.7, equivalent to a range of k_{22} from 3.8×10^4 M^{-1} s^{-1} to 8.3×10^6 M^{-1} s^{-1}.

K_{12}:

K_{12} is determined as 400 (± 50) from the UV-vis titrations described earlier. The uncertainty is calculated by propagating the error of three separate titration experiments. Each titration comprises 10 or more data points (spectra) where K_{12} is determined (*i.e.* K_{12} is determined after every addition of $[Fc]^+$ to $[LCu^{II}(OH)]^-$). This gives us good confidence in the robustness of both the reported K_{12} and its associated uncertainty.

k_{11}:

$$k_{11} = (k_{12}W_{12})^2 k_{22}K_{12}f_{12} \qquad \text{eq. S22}$$

Rearranging eq. S5 gives eq. S22. The uncertainties associated with the work term (W_{12}) and the frequency factor (f_{12}) are likely small. f_{12} has the value 1.0 which is quite insensitive to changes in its components. The uncertainties in W_{12} are likely in the radii and the hard-sphere assumption, which should be much smaller than the uncertainty in k_{12} or k_{22}. Thus, W_{12} and f_{12} have an insignificant contribution to the overall error of k_{11}.

The three terms in equation S22 with greatest uncertainty are k_{12}, k_{22} and K_{12}, and the above analysis shows that the dominant uncertainty is in k_{22}, the ferrocene self-exchange rate constant at 185 K. This

uncertainty is best estimated as ±2.7 in ln(k_{11}), following the discussion above. Propagating the uncertainties in k_{12}, k_{22} and K_{12} through equation S22 gives k_{11} = 3 (±8) × 10^4 $M^{-1}s^{-1}$.

Z:

The collision frequency is set as 10^{11} $M^{-1}s^{-1}$ in line with the diffusion limit in water.[6] Smaller values of Z may be used in organic solvent,[18] but the magnitude of this parameter has a negligible impact on k_{11} and likewise a negligible impact on λ. Indeed, the effect of a value Z < 10^{11} $M^{-1}s^{-1}$ in equation S23 is to further reduce λ. For example, if Z = 5 × 10^{10} $M^{-1}s^{-1}$ then λ = 0.91 eV, all other parameters being held constant.

λ:

$$k_{11} = Z \exp\left(\frac{-\lambda}{4RT}\right) \qquad \text{eq. S23}$$

$$\ln(k_{11}) - \ln(Z) = -\lambda/4RT \qquad \text{eq. S24}$$

Eq S23 can be rearranged to eq S24, giving the relationship between ln(k_{11}) and λ. The uncertainty in k_{11} of ±2.7 ln units thus translates into an uncertainty in λ of 2.7(4RT) = ±4.0 kcal mol^{-1} or ±0.17 eV. Overall, the uncertainties associated with each parameter of equations S22 and S23 do not change the conclusions of this work – that the reorganization energy is unusually small.

References

1 Maeder, M.; King, P. Reactlab, Jplus Consulting Pty Ltd: East Freemantle, WA. Australia, 2009.

2 Connelly, N. G.; Geiger, W. E., Chemical Redox Agents for Organometallic Chemistry. *Chem. Rev.* **1996**, *96* (2), 877-910.

3 Chávez, I.; Alvarez-Carena, A.; Molins*, E.; Roig, A.; Maniukiewicz, W.; Arancibia, A.; Arancibia, V.; Brand, H.; Manuel Manríquez, J., Selective oxidants for organometallic compounds containing a stabilising anion of highly reactive cations: $(3,5(CF_3)_2C_6H_3)_4B^-)Cp_2Fe^+$ and $(3,5(CF_3)_2C_6H_3)_4B+)Cp^*_2Fe^+$. *J. Organomet. Chem.* **2000**, *601* (1), 126-132.

4 Thomson, R. K.; Scott, B. L.; Morris, D. E.; Kiplinger, J. L., Synthesis, structure, spectroscopy and redox energetics of a series of uranium(IV) mixed-ligand metallocene complexes. *C. R. Chimie.* **2010**, *13* (6), 790-802.

5 Donoghue, P. J.; Tehranchi, J.; Cramer, C. J.; Sarangi, R.; Solomon, E. I.; Tolman, W. B., Rapid C–H Bond Activation by a Monocopper(III)–Hydroxide Complex. *J. Am. Chem. Soc.* **2011,** *133* (44), 17602-17605.

6 Marcus, R. A.; Sutin, N., Electron transfers in chemistry and biology. *Biochimica et Biophysica Acta (BBA) - Reviews on Bioenergetics.* **1985,** *811* (3), 265-322.

7 Eberson, L., *Electron Transfer Reactions in Organic Chemistry*. Springer-Verlag: Berlin, 1987; Reactivity and Structure: Concepts in Organic Chemistry, Vol. 25.

[8] Canzi, G.; Mrse, A. A.; Kubiak, C. P., *J. Phys. Chem. C.* Diffusion-Ordered NMR Spectroscopy as a Reliable Alternative to TEM for Determining the Size of Gold Nanoparticles in Organic Solutions. **2011**, *115* (16), 7972-7978.

[9] Morgan, S. O.; Lowry, H. H., *J.* Dielectric Polarization of Some Pure Organic Compounds in the Dissolved, Liquid, and Solid States. *Phys. Chem.* **1929,** *34* (11), 2385-2432.

[10] Tahsini, L.; Kotani, H.; Lee, Y.-M.; Cho, J.; Nam, W.; Karlin, K. D.; Fukuzumi, S., Electron-Transfer Reduction of Dinuclear Copper Peroxo and Bis-μ-oxo Complexes Leading to the Catalytic Four-Electron Reduction of Dioxygen to Water. *Chem. Eur. J.* **2012,** *18* (4), 1084-1093

[11] Nielson, R. M.; McManis, G. E.; Golovin, M. N.; Weaver, M. J., Solvent dynamical effects in electron transfer: comparisons of self-exchange kinetics for cobaltocenium-cobaltocene and related redox couples with theoretical predictions. *J. Phys. Chem.* **1988,** *92* (12), 3441-3450.

[12] Valkai, S.; Liszi, J.; Szalai, I., Temperature dependence of the refractive index for three chloromethane liquids at 514.5 nm and 632.8 nm wavelengths. *J. Chem. Thermodyn.* **1998,** *30* (7), 825-832.

[13] Uematsu, M.; Franck, E. U., Static dielectric constant of water and steam. *J. Phys. Chem. Ref. Data* **1981,** *9* (4), 1291-306.

[14] Linde, D. R., *Index of refraction of water / CRC Handbook of Chemistry and Physics*. CRC Press.: New York, 1995.

[15] Cao, R.; Saracini, C.; Ginsbach, J. W.; Kieber-Emmons, M. T.; Siegler, M. A.; Solomon, E. I.; Fukuzumi, S.; Karlin, K. D., Peroxo and Superoxo Moieties Bound to Copper Ion: Electron-Transfer Equilibrium with a Small Reorganization Energy. *J. Am. Chem. Soc.* **2016,** *138* (22), 7055-7066.

[16] Bard, A. J.; Faulkner, L. R., *Electrochemical Methods: Fundamentals and Applications*. 2 ed.; John Wiley & Sons, Inc.: New York, 2001.

[17] Shih Yang, E.; Chan, Man-Sheung.; Wahl, A., Electron Exchange between Ferrocene and Ferrocenium Ion. Effects of Solvent and of Ring Substitution on the Rate. *J. Phys. Chem*. **1980**, *84*, 3094-3099

[18] Kikuchi, K.; Sato, C.; Watabe, M.; Ikeda, H.; Takahashi, Y.; Miyashi, T., New aspects of fluorescence quenching by molecular oxygen. *J. Am. Chem. Soc*. **1993**, *115* (12), 5180-5184.